JOURNAL OF GEOPHYSICAL RESEARCH, VOL. 100, NO. D2, PAGES 3221–3232, FEBRUARY 20, 1995

Intercomparison between two satellite-based products of net surface shortwave radiation

Zhanqing Li

Canada Centre for Remote Sensing, Ottawa, Ontario, Canada

Abstract. This study compares two global satellite-based surface radiation budget (SRB) data sets as a means of quality evaluation. One was developed from Earth Radiation Budget Experiment (ERBE) satellite data using the algorithm of Li et al. (ERBE/SRB), and the other was generated by applying the algorithm of Pinker and Laszlo to International Satellite Cloud Climatology Project (ISCCP/SRB) data. The comparison is limited to net surface shortwave radiation (NSSR). The global annual mean of NSSR obtained from the two data sets differ by 15 W m^{-2}, and maximum regional differences exceed 100 W m^{-2}. The differences are investigated in terms of discrepancies in both input data and algorithm. It was found that large regional differences in SRB are associated mainly with the discrepancies in the input parameters, namely, top-of-atmosphere (TOA) flux and precipitable water. Differences in TOA flux between ERBE and ISCCP are attributed to angular and spectral corrections for ISCCP data and to different sampling in time and space by ERBE and ISCCP. ISCCP/SRB underestimates NSSR by 20–30 W m^{-2} over some dry regions arising from excessive amounts of precipitable water from the TIROS operational vertical sounder. Deficient treatment of aerosol in the Li et al. algorithm results in too large NSSR for the major deserts. Systematic discrepancies are accounted for by different methods to compute water vapor absorption. According to the line-by-line results, water vapor absorption was significantly underestimated by the Lacis and Hansen parameterization (used by Pinker and Laszlo) and is moderately overestimated by LOWTRAN 6 (used by Li et al.). If both algorithms use the same water vapor absorption scheme and the same input data, their global annual mean of NSSR agree to within 1 W m^{-2}. On the basis of these findings, some recommendations are made for future improvements of the two products. Overall, it appears that the quality of ERBE/SRB is superior to that of ISCCP/SRB (version 1.1).

1. Introduction

Surface radiation budget (SRB) is the major component of the Earth's surface energy balance. SRB is controlled by many complex climatic processes and feedbacks involving clouds, the atmosphere, and the surface of the Earth. Thus SRB can be a very useful parameter serving to diagnose a global climate model (GCM) with respect to the treatments of the above complex processes and feedbacks [*Barker and Li*, 1994; *Vardavas and Koutoulaki*, 1995]. Unfortunately, differences of up to 40 W m^{-2} were found among the state-of-the-art values of global annual mean net surface solar radiation (NSSR) obtained from surface observation, satellite estimation, and GCM simulation [*Li and Barker*, 1994]. The maximum discrepancy is more than 10 times the surface radiative perturbation due to doubling CO_2 [*Cess et al.*, 1993]. Yet, all the three leading GCMs that were investigated generate larger amounts of NSSR than those based on surface observation and satellite estimation [*Li and Barker*, 1994]. Recent studies using surface radiation measurements [*Garratt*, 1994; *Wild et al.*, 1995] also showed that many current GCMs compute excess solar radiation at surface. Correction for such an overestimation could lead to appreciable modifications to the treatments of these processes in GCMs [*Barker and Li*, 1994]. In addition to the applications for improving simulation of atmospheric circulation, SRB can also serve as boundary forcing for oceanic modeling [*Seager and Blumenthal*, 1994].

The general requirement for SRB in climate studies is to obtain the global monthly mean SRB data at the resolution of 250 km with an accuracy of 10 W m^{-2} [*Suttles and Ohring*, 1986]. Meeting this goal has been hampered by the lack of adequate surface observations. Although there are approximately 2000 stations operating worldwide equipped with radiometers, most stations are unevenly distributed over land and almost none are over the oceans [*Ohmura and Gilgen*, 1993]. The problem is exacerbated by the fact that only one tenth of the stations observe upwelling solar flux at the surface (surface albedo). Each of these measurements is merely representative of a few square meters [*Barker and Davies*, 1989a]. To circumvent these obstacles, retrieval of the SRB from satellite observations was initiated soon after meteorological satellites were launched [*Fritz et al.*, 1964]. The endeavor has been strengthened since the establishment of the SRB climatology project under the World Climate Research Program (WCRP) in the mid 1980s, with promising achievements made for shortwave (SW) SRB [*Schmetz*, 1989; *Pinker et al.*, 1995]. Global climatologies of all three SW radiative variables, namely, insolation, albedo, and

Published in 1995 by the American Geophysical Union.

Paper number 94JD02687.

absorbed radiation (i.e., NSSR) have been obtained from satellite data.

Because of the nature of retrieval, satellite-based estimates of the SRB are subject to thorough and rigorous quality evaluation. Although most of the satellite products have been, to a certain degree, validated against ground truth data, all validations suffer from the limited number of surface measurements and the difficulties in acquiring simultaneous and collocated satellite and surface measurements. Almost no validations were done over oceans and polar regions because of extreme paucity of surface measurements. Validation of NSSR is especially difficult, since surface albedo observations are scarce and of poor spatial representation. In view of these limitations, intercomparison of independent satellite products may be a useful alternative to shed light on the quality of the products.

This study compares two independent satellite-based SRB data sets. One was developed from the International Satellite Cloud Climatology Project (ISCCP) data using the algorithm of Pinker and Laszlo (ISCCP/SRB) and the other from the Earth Radiation Budget Experiment (ERBE) data using the algorithm of Li et al. (ERBE/SRB). While both data sets are for multiyear, the diagnostic study presented here is focused on two typical months in 1986 (January and July). The study is also restricted to NSSR, because the ERBE/SRB does not contain upwelling and downwelling components. Descriptions of the two data sets are given in section 2. Section 3 compares the two data sets and investigates the causes of their differences so as to identify the deficiencies of both products. Conclusions and recommendations for future improvements of the two data sets are given in section 4.

2. Data

2.1. International Satellite Cloud Climatology Project/ Surface Radiation Budget (ISCCP/SRB)

ISCCP/SRB data were generated at the NASA Langley Research Center. The first official release of ISCCP/SRB (version 1.1) was made recently for the period March 1985 through December 1988, designated as the First WCRP SRB Data [*Charlock et al.*, 1993]. The ISCCP/SRB data contain 52 parameters for monthly products and 10 for daily products [*Whitlock et al.*, 1993], including insolation, albedo, and net solar radiation. The data were derived mainly from ISCCP C1 data which has 6596 cells of equal area 280 × 280 km^2. The main advantage of using ISCCP data is that ISCCP offers more than 10 years of global cloud and radiation data deduced from operational meteorological satellites [*Schiffer and Rossow*, 1983]. In addition, information regarding the conditions of the atmosphere and surface are also included in ISCCP. Some of them were also employed in the generation of ISCCP/SRB, such as the TIROS operational vertical sounder (TOVS) precipitable water data. The ISCCP/SRB version 1.1 data were produced using two SW algorithms developed by *Pinker and Laszlo* [1992] (hereinafter referred to as the Pinker algorithm), and by Staylor [*Darnell et al.*, 1992]. They were selected initially among many algorithms participating in the validation campaigns which used observational data from some field experiments and radiation network stations [*Whitlock et al.*, 1990; *DiPasquale and Whitlock*, 1993]. At the GEWEX SRB Workshop held in Williamsburg, Virginia, November 10–12, 1993, a single algorithm of Pinker's was selected for future SRB processing. Therefore this paper only presents results for the Pinker algorithm. The algorithm was developed originally by *Pinker and Ewing* [1985] and improved later by *Pinker and Laszlo* [1992]. It is basically a tabulated relationship between broadband top-of-atmosphere (TOA) reflectivity and atmospheric transmissivity for specific atmospheric and surface conditions. The relationship was established by means of radiative transfer calculations using the delta-Eddington approximation. To apply the algorithm, it is required to identify clear-sky measurements, determine surface albedo and aerosol optical depth for cloud-free measurements, and retrieve cloud optical properties for cloudy pixels.

2.2. Earth Radiation Budget Experiment/SRB (ERBE/SRB)

Global monthly mean ERBE/SRB data were derived from ERBE S-4 TOA solar fluxes and column-integrated water vapor (or precipitable water) data from the European Centre of Medium-Range Weather Forecasting (ECMWF) analyses by *Li and Leighton* [1993] using the algorithm of *Li et al.* [1993a] (hereinafter referred to as the Li algorithm) at the resolution of 2.5° × 2.5° latitude/longitude. ERBE/SRB contains monthly mean NSSR data from January 1985 through December 1989. Although ERBE data are available for a shorter period than ISCCP data, the former are well-calibrated broadband measurements as opposed to the lack of onboard-calibrated narrowband measurements of the latter [*Barkstrom et al.*, 1989]. Narrowband to broadband conversion is thus unnecessary with ERBE data, which eliminates a major potential error source [*Li and Leighton*, 1992]. Moreover, ERBE has a set of angular dependence models (ADMs) to convert radiance into irradiance and to derive daily mean quantities from instantaneous quantities [*Suttles et al.*, 1988; *Smith et al.*, 1986]. In addition to the discrepancies in input data, Li's algorithm is very different from Pinker's. The Li algorithm estimates directly the monthly mean NSSR without resorting to any information regarding surface, clouds, and atmospheric conditions [*Li et al.*, 1993a]. The algorithm is a simple linear relationship that relates NSSR to the reflected flux at the top of the atmosphere with its coefficients being functions of precipitable water and cosine of the solar zenith angle. It was derived on the basis of comprehensive radiative transfer simulations for a variety of atmospheric, cloud, and surface conditions. The algorithm was tested using collocated surface measurements made at two meteorological towers and those obtained simultaneously from ERBE satellites [*Li et al.*, 1993b].

2.3. Validation Against Ground Truth

Both satellite products were compared to the Global Energy Balance Archive (GEBA) [*DiPasquale and Whitlock*, 1993; *Li et al.*, 1995]. GEBA is a world-wide data base containing 150,000 station months of monthly mean fluxes at up to 1600 sites [*Ohmura and Gilgen*, 1991]. The main source of radiation data is the worldwide surface radiation network. The original point-based GEBA data were aggregated into ISCCP C1 cells and the cell mean radiative fluxes were included in ISCCP/SRB. ERBE/SRB data were also converted from 2.5° × 2.5° grids into ISCCP C1 cells using a two-dimensional Lagrangian interpolation scheme. The validation was done for surface downwelling insolation, owing to the problem with GEBA surface albedo. To obtain surface insolation from ERBE/SRB, a global surface albedo data set derived independently by Staylor was employed [*Li et al.*,

1995]. Table 1 presents validation results for four GEBA subsets of varying quality and number of surface sites in an ISCCP C1 cell [*Li et al.*, 1995]. The German subset was considered most reliable and contains seven or more surface sites. It follows that the ERBE/SRB estimates agree very favorably with GEBA observations in terms of mean bias error. The ISCCP/SRB estimates are systematically larger than surface observations by moderate amounts. In comparison, random errors are much higher for both satellite data sets. However, the fact that the random error decreases significantly with increasing density of the surface sites suggests that the random error is partly associated with inadequate spatial sampling. *Li et al.* [1995] demonstrated that the "real" random error for an infinitive number of surface stations would be approximately 5 W m^{-2}.

3. Intercomparison

A direct way to compare two data sets is to compute their differences. Plate 1 shows the difference in NSSR between ERBE/SRB and ISCCP/SRB for January and July 1986. Note that red (blue) colors of various tints represent that the ISCCP/SRB values are larger (lower) than the ERBE/SRB ones by varying amounts. The most striking feature of Plate 1 is that the majority of areas are red, indicating that the NSSR values from ISCCP/SRB are systematically larger than those from ERBE/SRB. The largest differences occur in polar regions where the former are larger than the latter by 35–112 W m^{-2}. Over the western Pacific and nearby East Asia (GMS region) the former are larger than the latter by 25–45 W m^{-2}. Over the majority of areas, positive differences are of the order of 10 W m^{-2}. There are a few confined regions where the ISCCP/SRB values are less than the ERBE/SRB ones, such as the Southeast Pacific and South America in January and western Europe, the Arabian countries, and the bounds of the African continent in July. However, positive differences dominate over negative ones in terms of both magnitude and occurrence frequency, as is shown in the histograms of the differences (Figure 1). The bars of larger than 35 W m^{-2} correspond to the cases with maximum regional differences. The difference in global mean NSSR between ERBE/SRB and ISCCP/SRB is approximately 15 W m^{-2} for both months.

As the two products were obtained from different input data and algorithms, differences in NSSR between ISCCP/SRB and ERBE/SRB lie in the discrepancies in both input data and algorithm. To separate the contribution of the two factors, the Li algorithm was applied to the ISCCP TOA data and TOVS precipitable water data. The resulting NSSR data were then subtracted from the ERBE/SRB and ISCCP/SRB values. The former and latter differences stem from input data and algorithm, respectively.

Table 1. Comparison of Surface Solar Irradiance Obtained From Satellite Estimation and Surface Observation

SRB Data Set	Total GEBA Set	GEBA Subset	Multisite Subset	German Subset
ERBE/SRB	0.3 (27.5)	−2.4 (25.1)	−2.4 (14.9)	0.8 (8.1)
ISCCP/SRB	10.1 (25.1)	7.1 (21.4)	7.9 (17.4)	5.8 (7.6)

Bias and random errors (W m^{-2}) are given outside and inside parentheses, respectively [after *Li et al.*, 1994]. SRB, surface radiation budget; GEBA, Global Energy Balance Archive; ERBE, Earth Radiation Budget Experiment; ISCCP, International Satellite Cloud Climatology Project.

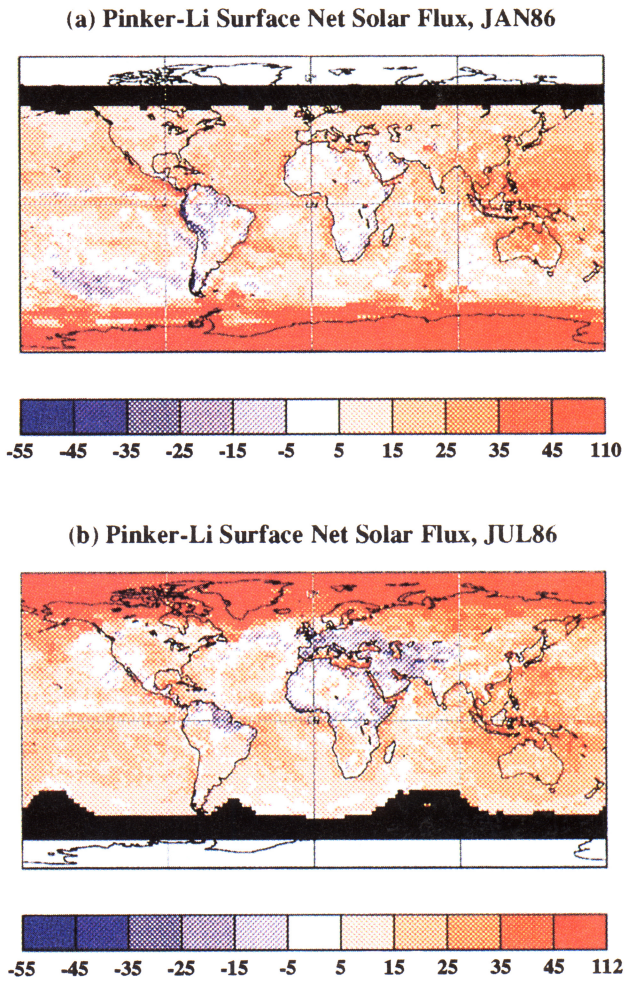

Plate 1. Differences in net surface shortwave radiation (watts per square meter (W m^{-2})) between the Earth Radiation Budget Experiment/surface radiation budget (ERBE/SRB) and the International Satellite Cloud Climatology Project (ISCCP)/SRB for (a) January and (b) July 1986. The limiting values on the legend bar are extremes in the plot. Black color represents missing data for ISCCP/SRB.

3.1. Differences Due to Input Data

Plate 2 depicts the difference in NSSR due to the use of different sets of input parameters. In contrast to Figure 1, Plate 2 shows no dominant colors, suggesting that different input data do not account for the systematic discrepancies between ERBE/SRB and ISCCP/SRB. However, Plate 2 does show a lot more striking spatial patterns, indicating that the differences in input data are responsible for the large regional differences. Some important regional features shown in Plate 2 are difficult to see in Plate 1, implying that errors due to input data and algorithm may offset each other over some areas. One interesting feature that stands out in Plate 2 is the blue circle around Africa in July, which demarcates the edge of the Meteosat coverage. Also, the coverage of GOES is more visible in Plate 2 than in Plate 1. These features indicate that ISCCP/SRB data have a depen-

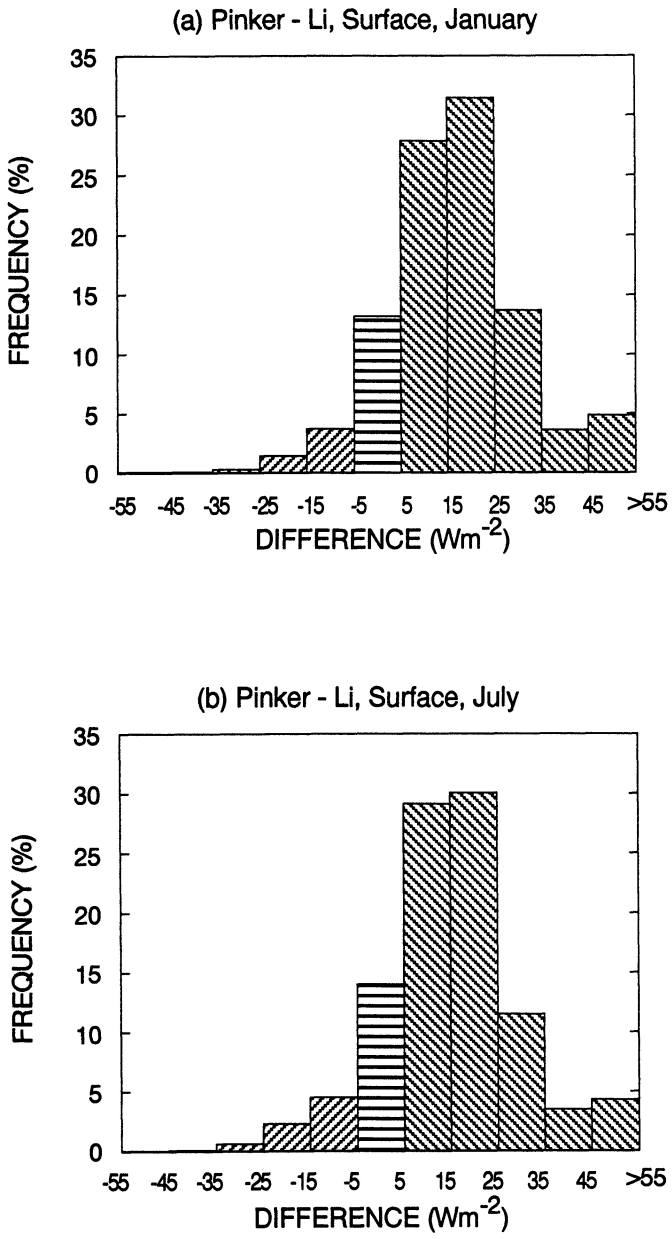

Figure 1. Histograms of the differences (W m^{-2}) in net surface shortwave radiation between ERBE/SRB and ISCCP/SRB.

dence on viewing angle. As the input data include both TOA fluxes and precipitable water amounts, it is necessary to investigate their effects separately.

TOA measurements made from spaceborne platforms are the most important input data for all retrieving methods. Since the ISCCP TOA data are narrowband quantities obtained from operational satellites, the Pinker algorithm infers TOA broadband quantities using a narrowband-to-broadband conversion scheme. Besides, the ERBE ADMs were employed to conduct angular corrections for the ISCCP reflected fluxes at TOA. Differences in TOA net solar fluxes between ERBE and ISCCP are shown in Plate 3. It appears that the distribution of Plate 3 is very similar to that of Plate 2. Some of the differences in TOA net solar radiation can be attributed to angular and spectral corrections for the ISCCP TOA data. Negative differences (blue areas) over the edges of the Meteosat and GOES coverage are presumably related to angular correction. It should, however, be pointed out that the satellite coverage is not discernible in the distribution of ISCCP TOA fluxes but in that of their differences with ERBE data. This may indicate that the problem arises from the combining effects of imperfect ADMs and a nonuniform number of samples for ISCCP data with respect to satellite viewing angle (R. T. Pinker, private communication, 1994). On the other hand, positive differences over the polar regions and large portions of the continents are associated with spectral conversion. It appears that the conversion scheme introduces an error dependent on surface albedo. The higher the albedo the larger the net TOA solar flux is overestimated. Over the oceans the conversion scheme works fairly well. Maximum overestimation is found over deserts and polar regions. This is presumably due to the fact that cloud identification is subject to larger errors over the regions of higher surface albedo (low clear/cloud contrast) and that the narrowband-to-broadband conversion depends strongly on scene type [*Li and Leighton*, 1992]. This is particularly true in the polar areas where the ISCCP scheme

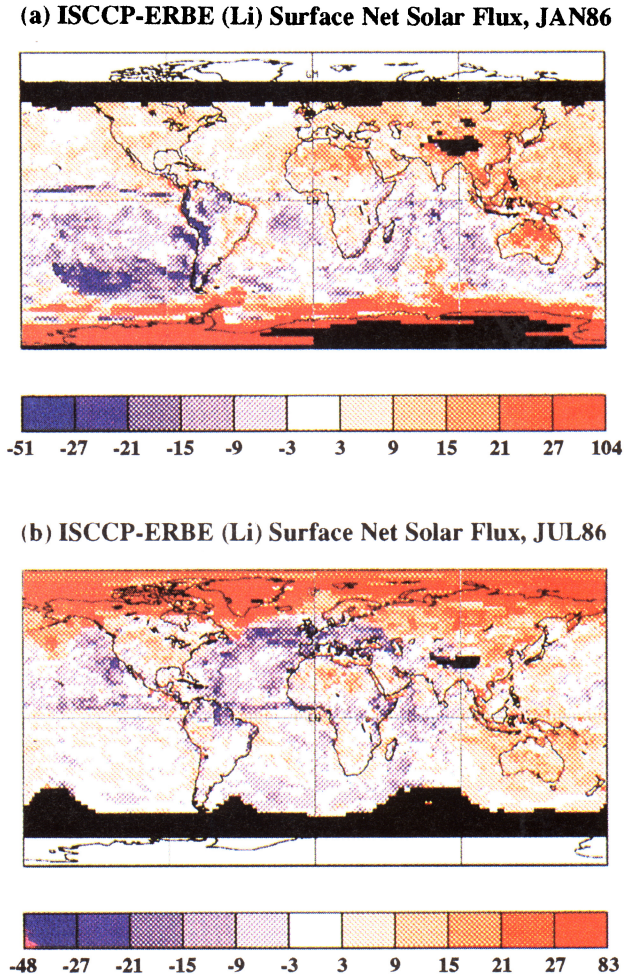

Plate 2. Differences in net surface shortwave radiation (W m^{-2}) caused by different input data for (a) January and (b) July 1986. They are obtained by applying the Li algorithm to the ISCCP data and subtracting the resulting values from the ERBE/SRB data.

does not effectively distinguish clouds from the clear bright snow/ice surfaces. On the other hand, the spectral conversion for snow/ice differs considerably from that for clouds because of different spectral dependencies of their reflectivities. It is worth noting that ISCCP is reprocessing polar data by adding channel 3 of the advanced very high resolution radiometer (AVHRR) to improve cloud identification (W. B. Rossow, private communication, 1994). Of course, the TOA data of ERBE are not free of errors in the polar regions. In fact, ERBE-reflected fluxes have larger uncertainties at high latitudes than in low latitudes. This is because the ERBE ADMs perform worst in polar summer when the existence of ponds, leads, etc., deteriorates considerably the efficiency of the ERBE snow ADM [*Li*, 1991]. The problem is exacerbated by ERBE's poor scene identification over snow/ice surfaces [*Li and Leighton*, 1991]. Correct scene identification is necessary for selecting an appropriate ADM to derive a reflected flux from a radiance measurement. In a word, both ERBE/SRB and ISCCP/SRB have potential large errors in polar regions. Quantitative estimates of the uncertainties await validation against ground truth observations.

When examining the global mean, however, the TOA difference does not contribute to the systematic differences in NSSR between ERBE/SRB and ISCCP/SRB. Figure 2 presents a frequency histogram of the differences shown in Plate 3. In contrast to Figure 1, Figure 2 exhibits much more symmetrical distributions with respect to zero difference. Yet, 45% of the differences are less than 5 W m^{-2} in magnitude. The global mean differences in TOA net flux are 0.3 and -1.0 W m^{-2} for January and July, respectively. The discrepancies in NSSR due solely to different TOA data can be obtained by computing the differences between ERBE/SRB and the NSSR derived by applying the Li algorithm to the ISCCP-based TOA broadband fluxes and ECMWF precipitable water data. As expected, the distribution patterns of the differences (not shown) are almost identical to those shown in Figure 4 except the magnitudes are proportional to the TOA differences.

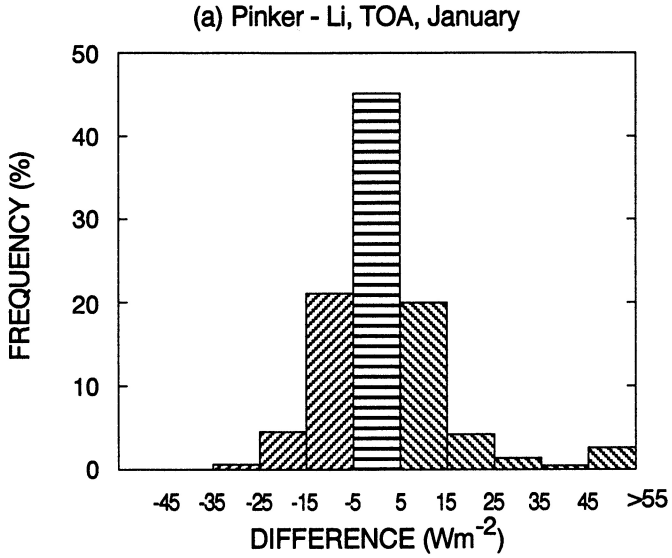

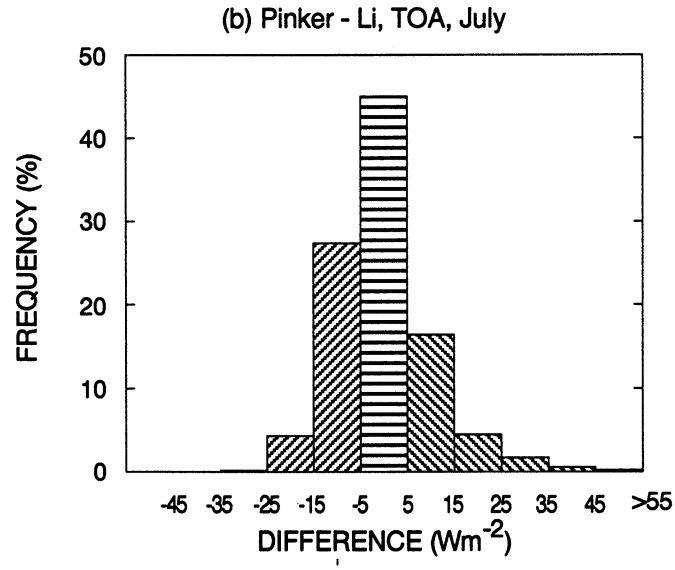

Figure 2. Histograms of the differences in TOA net solar flux between ERBE and ISCCP.

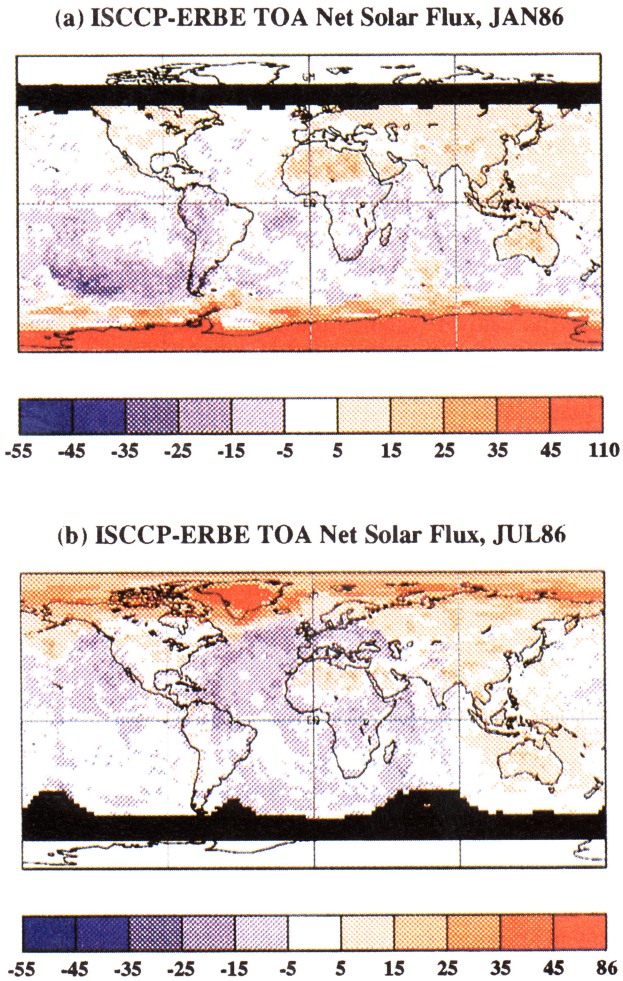

Plate 3. Differences in top-of-atmosphere (TOA) net solar flux (W m^{-2}) obtained from ERBE and ISCCP for (a) January and (b) July 1986. The broadband ISCCP TOA fluxes are inferred from narrowband data using the Pinker algorithm.

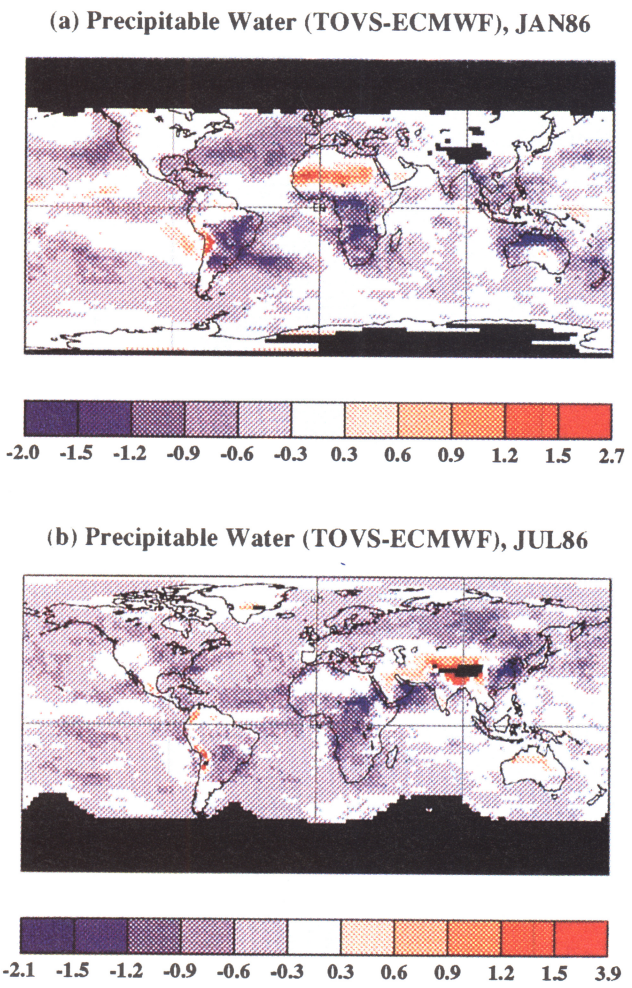

Plate 4. Differences in precipitable water (centimeters) obtained from the European Centre for Medium-Range Weather Forecasts and TIROS operational vertical sounder (TOVS) for (a) January and (b) July 1986.

Precipitable water is another input parameter used in the two algorithms. Sensitivity study indicates that NSSR depends moderately on precipitable water [*Li et al.*, 1993a, b]. Although ECMWF water vapor data are different from the TOVS data, they are not completely independent; the latter being routinely assimilated into the former. Apart from TOVS, the ECMWF water vapor data also incorporate global radiosonde observations, microwave data from satellites, and modeling results. As the ECMWF data were given at 2.5° × 2.5° latitude and longitude grids, they were also converted into an equal-area format in order to be compared with the TOVS data. Plate 4 presents the differences in precipitable water between ECMWF and TOVS. It is seen that precipitable water agrees to within 0.6 cm in most areas, with a global mean difference of 0.4 cm for both months. Except for a few isolated areas, TOVS water vapor content tends to be lower than the ECMWF. The blue areas in January coincide approximately with the major cloud systems such as the winter storms, Intertropical Convergence Zone, etc., while in July they appear to be more dispersed. There are a few areas over land where precipitable water from TOVS is considerably higher than that from ECMWF by amounts reaching 2.62 cm in January and 3.94 cm in July. These areas correspond to relatively dry areas, including major deserts such as the Sahara, the Saudi, the Gobi, and the Gibson and highlands such as the Tibetan Plateau and the Andes Mountains. Over these regions the distribution of precipitable water from the ECMWF is in sharp contrast to the surroundings as expected [see *Li and Leighton*, 1993, Figure 2] whereas the distribution from the TOVS shows no or very little spatial variation.

The difference in precipitable water may lie in the errors of the ECMWF data, the TOVS data, or both. While ground truth data from radiosonde are insufficient to attribute the above differences, physical consideration lends more support to the ECMWF data than to the TOVS data for the regions of positive differences. It is generally recognized that precipitable water can be retrieved more accurately from microwave measurements than from TOVS. Unfortunately, the microwave retrieval techniques have been restricted to oceans only [e.g., *Liu et al.*, 1992], because of the difficulty in determining land emissivity. Comparison between precipitable water from the special sensor microwave/imager (SSM/I), ECMWF, and TOVS shows that precipitable water amounts from SSM/I agrees well with those from ECMWF and TOVS over most ocean areas. However, substantial discrepancies of up to 2 cm were found over very dry regions such as the upwelling regions of cool oceans and very wet regions including ITCZ, IPCZ, for both ECMWF and TOVS water vapor data, in comparison to the microwave results that agree well with radiosonde observations available in these areas. Nevertheless, the values of ECMWF are closer to those of SSM/I than the TOVS data [*Liu et al.*, 1992].

To investigate the difference of NSSR resulting from different precipitable water data, the precipitable water data from ECMWF and TOVS were employed together with the same TOA flux data to estimate NSSR using the Li algorithm. Again, as expected, the distribution of the difference of NSSR (not shown) exhibits the same pattern as that for precipitable water. Overall, use of the TOVS precipitable water yields larger NSSR. In most areas the overestimation is less than 5 W m^{-2} and the global mean difference is 2.5 W m^{-2}. However, differences of up to 22 W m^{-2} in January and 31 W m^{-2} in July occur over some dry areas where too high precipitable water from TOVS leads to NSSR being underestimated substantially in the ISCCP/SRB.

In general, the effects of TOA flux differences outweigh those of precipitable water. However, the impacts of the differences in precipitable water may ameliorate or exacerbate the discrepancies due to the TOA differences. For example, the two effects have opposite signs and thus they counteract each other over the major deserts and the southern edge of the GOES coverage, whereas their signs are the same and thus the two effects are added over the western Pacific, Southeast Asia, and around Australia and over large areas of Eurasia.

3.2. Differences Due to Algorithms

Plate 5 presents the difference of NSSR resulting from different algorithms. It was obtained by applying the Li algorithm to the ISCCP TOA broadband data and TOVS precipitable water data and the resulting NSSR values were subtracted from the ISCCP/SRB. In contrast to the irregular patterns exhibited in previous figures, the distribution of Plate 5 is basically zonal for oceans and interrupted by continents. Except for major deserts, positive differences

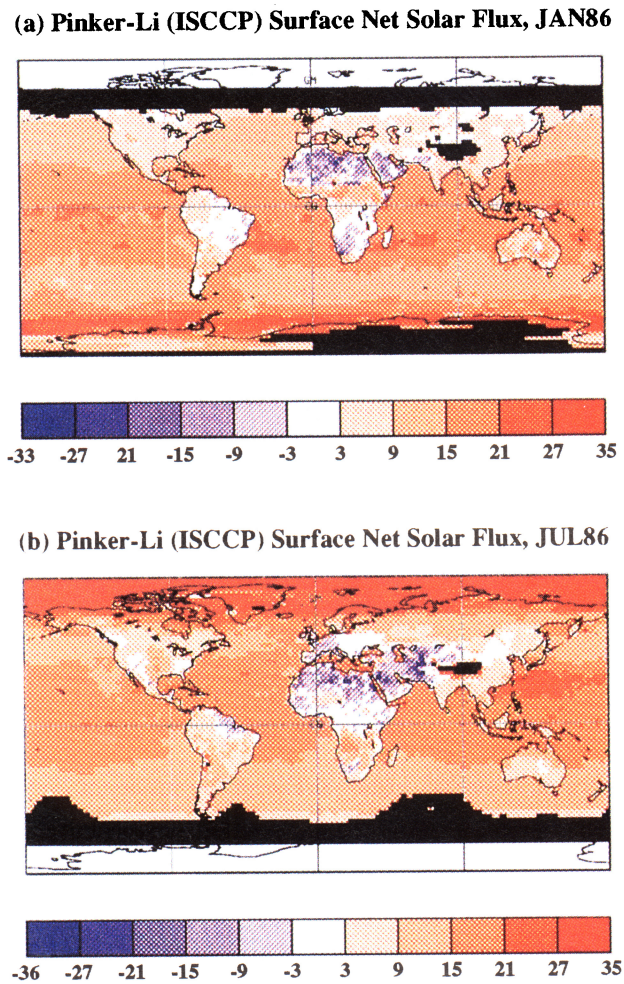

Plate 5. Differences in net surface shortwave radiation (W m^{-2}) obtained by applying the algorithms of Li and Pinker to the same input data (ISCCP) for (a) January and (b) July 1986.

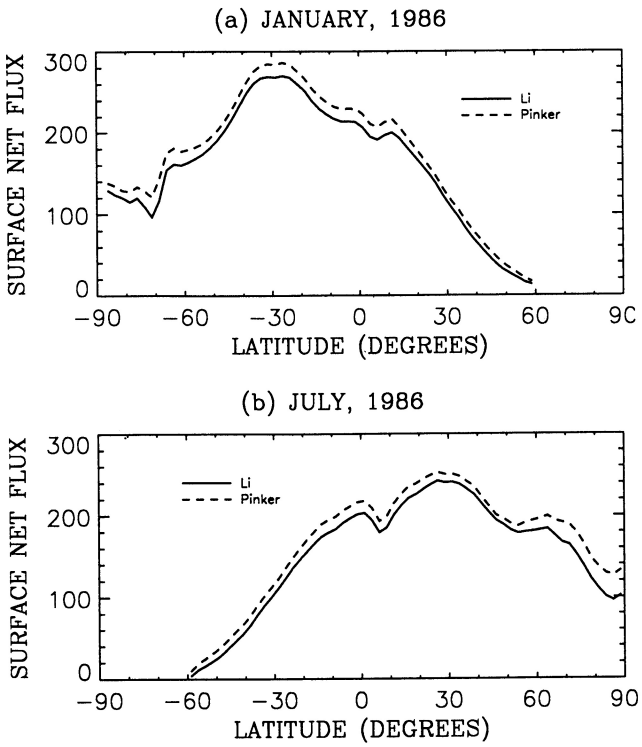

Figure 3. Comparison of zonal mean net surface shortwave radiation (W m^{-2}) obtained by applying the algorithms of Li and Pinker to the same input data (ISCCP) for (a) January and (b) July 1986.

are found everywhere, indicating that the Pinker algorithm yields systematically higher NSSR than the Li algorithm. The difference amounts to 35 W m^{-2}, with a global mean of 12.4 W m^{-2} for January and 11.9 W m^{-2} for July. The distribution pattern shown in Plate 5 bears a strong resemblance to that of clear-sky surface net solar flux as opposed to that for all skies [*Li and Leighton*, 1993]. This is surprising since the differences are for all-sky conditions and that the two algorithms treat cloud in a completely different manner. The Li algorithm does not treat cloud explicitly as it requires no cloud information, whereas the Pinker algorithm is driven mainly by retrieved cloud parameters. This is another indication that the Li algorithm can effectively take into account the impacts of clouds without including them, insofar as the way they are dealt with by Pinker is correct. The finding suggests that the systematic differences are not caused by the treatment of clouds but rather by clear-sky calculations. Yet, the same input at the TOA further eliminates the possibility that the difference is associated with atmospheric reflection. Thus it is concluded that the systematic difference in the estimation of NSSR is mainly due to differences in the computation of clear-sky atmospheric absorption. As Plate 5 exhibits a strong zonal pattern, the ensuing discussions are restricted to zonal mean quantities. Figure 3 presents the comparison of zonal mean NSSR shown in Plate 5.

Since water vapor absorption plays a major role in atmospheric absorption, the schemes used to compute water vapor absorption are compared. LOWTRAN 6 was employed in the development of the Li algorithm [*Li et al.*, 1993a], whereas the parameterization of *Lacis and Hansen* [1974] was included in the Pinker algorithm. Table 2 compares the solar fluxes absorbed by water vapor for the middle-latitude summer atmosphere [*McClatchey et al.*, 1972] computed with the two schemes. For comparison, the table also gives the results of line-by-line (LBL) calculations conducted by Ramaswamy and Freidenreich [*Fouquart et al.*, 1991] and those of the modified Lacis-Hansen scheme developed by *Ramaswamy and Freidenreich* [1992]. It is clear that the original Lacis and Hansen scheme computes atmospheric absorption significantly lower than LOWTRAN

Table 2. Solar Atmospheric Absorption (W m^{-2}) by Water Vapor Only in Midlatitude Summer Atmosphere for Two Solar Zenith Angles With Surface Albedo of 0.2

	Solar Zenith Angle	
	30°	75°
Lacis-Hansen	162.3	63.6
LOWTRAN 6	185.8	73.3
LBL	178.1	71.4
Modified Lacis and Hansen	178.7	69.7

LBL, line by line. LBL and modified Lacis and Hansen results were taken from *Ramaswamy and Freidenreich* [1992].

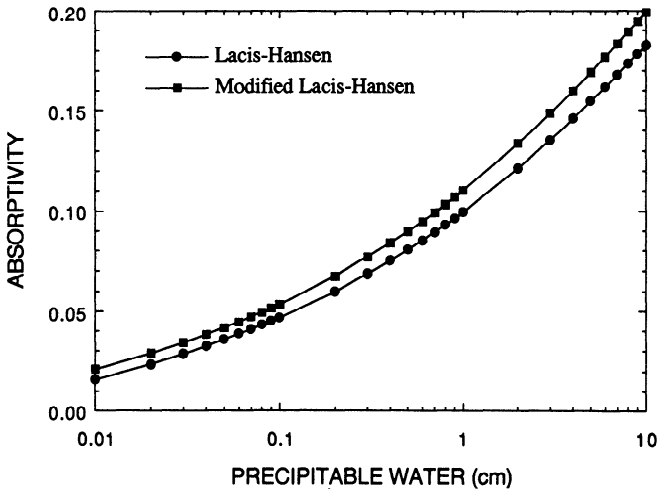

Figure 4. Comparison of the absorptivity computed by the original and modified Lacis-Hansen schemes for varying water vapor amounts.

6. With reference to the LBL results, atmospheric absorption is considerably too low by the Lacis and Hansen scheme and moderately too large by LOWTRAN 6. It is not surprising to note that the modified Lacis-Hansen results are very close to those of LBL calculations, since the modified Lacis-Hansen parameterization was derived from the LBL results [*Ramaswamy and Freidenreich*, 1992]. Figure 4 compares water vapor absorptivity using the original and modified Lacis-Hansen schemes for various water vapor amounts. It follows that the difference of water vapor absorptivity increases slightly with precipitable water.

Assuming that the LBL results are correct, it is possible to investigate errors in the ISCCP/SRB estimates of monthly mean NSSR due to the use of Lacis-Hansen's water vapor absorption. To do so, radiative transfer calculations were conducted with two water vapor absorption schemes, namely, the original and the modified Lacis-Hansen parameterizations. Clear-sky monthly mean NSSR was simulated for each latitude zone of 2.5° using zonal mean surface albedo and precipitable water from ISCCP/SRB as major input data. Figure 5 shows the latitudinal variation of the difference in NSSR obtained from the two schemes. Since the difference in absorptivity does not depend strongly on precipitable water, the difference in NSSR is mainly altered

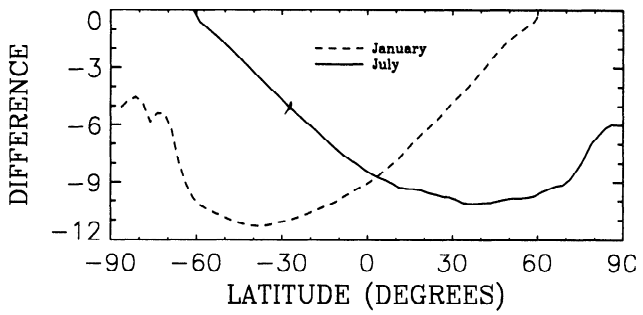

Figure 5. Zonal mean differences in daily mean net surface shortwave radiation (W m^{-2}) due to the use of the original and modified Lacis-Hansen schemes for clear condition. The difference is modified value minus original one.

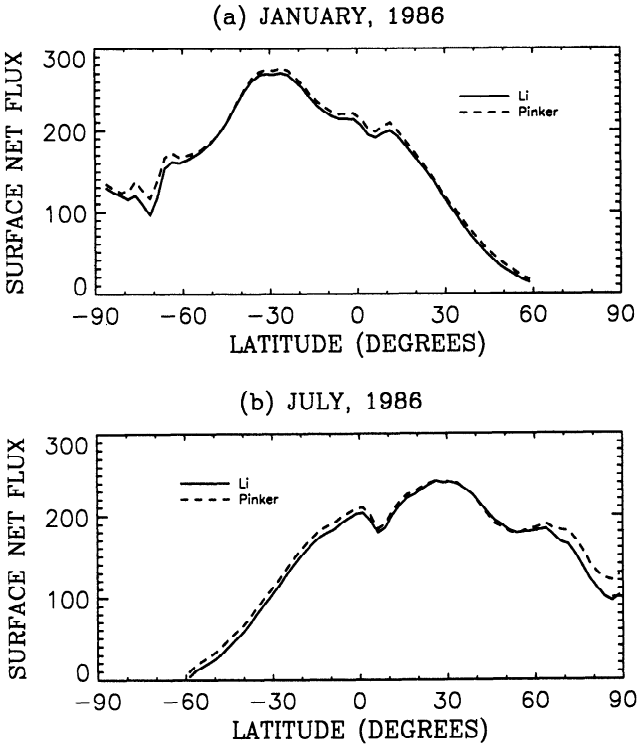

Figure 6. Same as Figure 3, except the results of Pinker are corrected for the computation of water vapor absorption according to the modified Lacis and Hansen scheme.

by TOA insolation and surface albedo. Relatively small differences over polar regions during the summer are attributed to high surface albedos. For all skies the differences should be close to those for clear skies except for highly reflective surfaces such as in polar regions. Over these areas, multiple reflections between clouds and surfaces enhance the differences. If the ISCCP/SRB estimates are deducted by the amounts given in Figure 5, the agreements between the ISCCP/SRB and the ERBE/SRB are improved significantly, as is shown in Figure 6 in comparison to Figure 3. The global mean difference is reduced to 5.0 W m^{-2} for both January and July.

Following the same procedure, the amounts of the NSSR overestimated by LOWTRAN 6 were also calculated. If the overestimated amounts are added to the estimates of NSSR obtained by applying the Li algorithm to the ISCCP data, the zonal mean values are almost in perfect agreement with the corrected ISCCP/SRB values (Figure 7). The global mean difference becomes less than 1 W m^{-2} for both months. However, the agreements over polar regions remain relatively poor. This is partly because multiple reflections are not accounted for in the computation and partly because the Li parameterization was developed from radiative transfer calculations with water vapor loadings greater than 1.1 cm. Precipitable water over polar regions are often well below this value. The algorithm has been modified to allow for, among others, extremely small amounts of precipitable water [*Masuda et al.*, 1995]. Preliminary investigation indicates that the original algorithm may overestimate monthly mean NSSR by amounts ranging from 5 W m^{-2} over the Arctic to 10 W m^{-2} over the Antarctic. The remaining

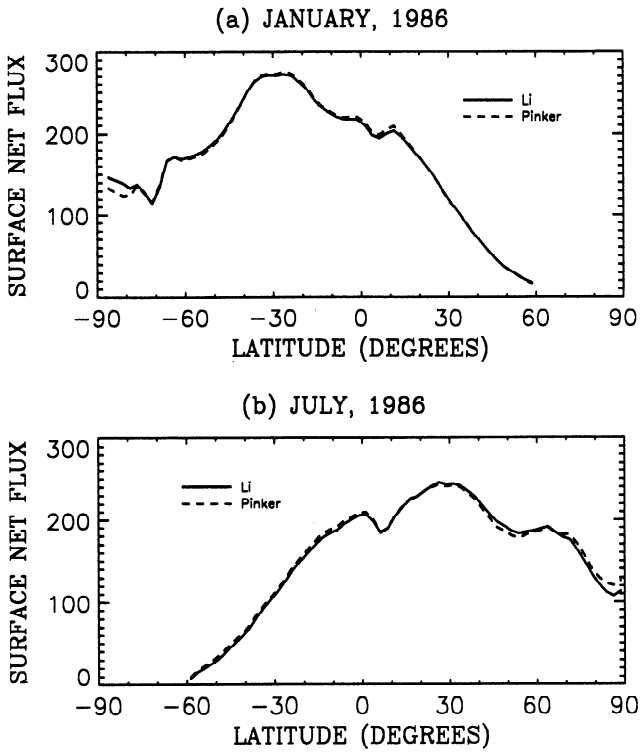

Figure 7. Same as Figure 6, except the results of Li are also corrected for the computation of water vapor absorption according to the modified Lacis and Hansen scheme.

amounts shown in Figure 7 are presumably due to the effects of multiple reflections.

While the distributions in Plate 5 are dominated by zonal patterns of positive differences which have been accounted for by different treatments of water vapor absorption, there appears to be systematic discrepancies between land and ocean, differences over land being smaller than over ocean. It is therefore expected that after correcting for water vapor absorption, the remaining differences will be negative over land and positive over ocean. The magnitudes of the remaining differences will be much smaller (<5 W m^{-2}) over most areas except the major deserts where the negative differences will be accentuated. The maximum difference over the Sahara, for example, might go below −40 W m^{-2}.

The discrepancies between ocean and land can be attributed to the treatment of aerosols. The aerosol type used in the development of the Li algorithm is the Arctic haze model of *Blanchet and List* [1983] with an optical depth of 0.05 at 0.55 μm. The Pinker algorithm employs two atmospheric aerosol profiles: MAR-I for the oceans and CONT-I for the land defined in *World Climate Program* (*WCP-55*) [1983] (R. T. Pinker, private communication, 1994). Figure 8 compares the single-scattering albedos of the three aerosol types. Note that CON-I and MAR-I are stronger and weaker absorbers for wavelengths less than 2.5 μm (containing 96% of the total solar energy at the TOA), respectively, relative to the Arctic aerosol. Therefore in comparison to the incorporation of CON-I over land and MAR-I over ocean, use of Arctic aerosol everywhere tends to overestimate (underestimate) NSSR over land (ocean). The finding that the ERBE/SRB estimates agree very well with surface measurements over land [*Li et al.*, 1995] may suggest that the overestimation

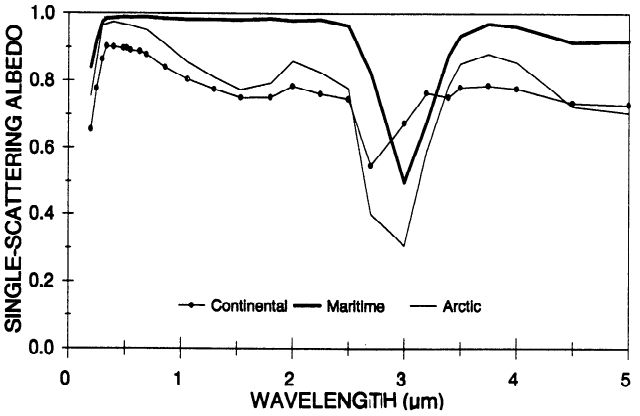

Figure 8. Comparison of single-scattering albedo for three types of aerosols.

related to aerosol is counteracted by the underestimation due to excessive water vapor absorption computed by LOWTRAN 6.

The magnitude of overestimation/underestimation depends on the optical depth of aerosol. This is clearly demonstrated in Figure 9 which shows the relationships between the reflected flux at the TOA and the absorbed flux at the surface for the same type of aerosol (CON-I) but of different optical depths (0.225, 0.5, and 1.0). The optical depth of 0.225 is supposed to represent the average continental aerosol (WCP-112). It is, however, realized that the optical depth over land regions may be significantly less than 0.225, especially for rural areas, whereas it is not unusual to observe optical depths larger than 1.0 over deserts [*D'Almeida*, 1987]. On the other hand, the variability of aerosol optical depth for a given season and location is much smaller than the range considered in Figure 9 over most land areas.

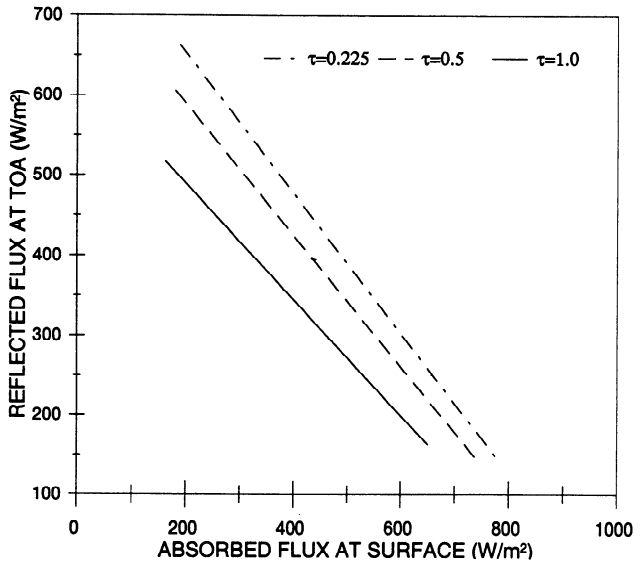

Figure 9. Relationship between reflected flux at the TOA and absorbed flux at the surface for CON-I aerosol of three optical depths given by τ. The straight lines join two points representing the results of calculations for surface albedos of 0.2 and 0.8 with a midlatitude summer atmosphere at solar zenith angle of 30° for varying aerosol optical loadings.

Regardless, Figure 9 suggests that aerosol optical depth should be treated explicitly. The effects of aerosol may have been overlooked in the Li algorithm. The optical depth used by the Pinker algorithm is retrieved for each clear day. Unfortunately, the retrieved optical depths were not archived in the ISCCP/SRB and the quality of the data has not been assessed. Quantitative evaluation of the differences due to aerosol effects is thereby precluded.

4. Concluding Remarks and Recommendations

Knowledge of surface radiation budget (SRB) is important for climate and oceanic modeling. Global data of SRB have been obtained from satellite measurements. As a part of quality analyses, a detailed investigation of the discrepancies in net surface shortwave radiation (NSSR) between two independent satellite-based SRB products was presented. One was developed from ERBE TOA irradiance data and ECMWF precipitable water data using the Li et al. algorithm (ERBE/SRB) and the other from ISCCP TOA radiance and cloud data and TOVS water vapor data employing the Pinker and Laszlo algorithm (ISCCP/SRB). The difference in the global annual mean NSSR between ERBE/SRB and ISCCP/SRB is approximately 15 W m^{-2}. Regional differences of up to 40 W m^{-2} occur in some low- and middle-latitude regions, and maximum differences of more than 100 W m^{-2} were found in polar regions. Since the two products were generated from different input data sets and algorithms, differences in NSSR were explained in terms of the discrepancies in algorithm and input data. To separate the two contributions, the Li algorithm was applied to ISCCP data and the resulting NSSR data were subtracted from the ERBE/SRB and ISCCP/SRB data. The former and latter differences are due to different input data and algorithm, respectively.

Large regional differences were found to be associated mainly with two input parameters, namely, TOA net radiative flux and column-integrated precipitable water. Most of the differences at the TOA between ERBE and ISCCP can be attributed to problems of angular and spectral corrections for ISCCP data. Some TOA differences are related to different sampling schemes used by ERBE and ISCCP. Problems in ERBE scene identification and angular dependence model also contribute to the TOA differences over polar regions. The TOA differences account for the majority of the large regional discrepancies in NSSR between ERBE/SRB and ISCCP/SRB, in particular, near the edges of the geostationary satellite coverage, and over highly reflective surfaces. They do not, however, contribute to systematic differences in NSSR between the two data sets. Unreasonably high precipitable water amounts over some deserts and the Tibetan Plateau from TOVS lead to NSSR being underestimated by 20–30 W m^{-2} in the ISCCP/SRB data.

Use of different algorithms explains the systematic discrepancies between ERBE/SRB and ISCCP/SRB. The performance of the two algorithms under study differs considerably in the computation of water vapor absorption. Relative to LBL calculations the Lacis and Hansen parameterization used by the Pinker and Laszlo algorithm underestimates significantly water vapor absorption, whereas the LOWTRAN 6 employed in the development of the Li et al. algorithm overestimates moderately. Two thirds of the systematic difference in NSSR between ERBE/SRB and ISCCP/SRB are due to the underestimation by the Pinker and Laszlo algorithm, while the remaining is due to the overestimation by the Li et al. one. If the two algorithms had the same water vapor absorption scheme and were applied to the same input data, their global annual mean NSSR values would agree to within 1 W m^{-2}. This is amazing, considering that the two algorithms are totally different. Regional differences can be, however, much larger.

If the effect of water vapor absorption is removed, the NSSR values from the algorithm of Li et al. tend to be slightly larger than those from that of Pinker and Laszlo over land and smaller over ocean. This can be explained by the fact that the aerosol used by Li is less absorbing over land and more absorbing over the oceans, relative to those used by Pinker. The good agreements between ERBE/SRB estimates and surface observations [*Li et al.*, 1994] may indicate that the overestimation due to aerosol effects over land happens to be counterbalanced by the underestimation due to water vapor absorption. Over major deserts the NSSR estimates from Li et al.'s algorithm are considerably lower than those from Pinker and Laszlo's with the same input data. This is due to the fact that the Li et al. algorithm used a constant optical depth (0.05) everywhere, whereas the Pinker algorithm retrieves optical depth for each region. Although the optical depth retrieved for the major deserts by the Pinker and Laszlo algorithm is more reliable, the NSSR values from ISCCP/SRB over these regions are also questionable. Three types of errors were identified for ISCCP/SRB over deserts, namely, overestimation of the TOA net solar fluxes, excessive precipitable water amounts, and errors in computing water vapor absorption. Besides, the values of surface albedo for the major deserts used by Pinker are significantly lower than the recent estimates from satellite observations [*Barker and Davies*, 1989b; *Staylor and Wilber*, 1990; *Arino et al.*, 1991; *Li and Garand*, 1994]. Unfortunately, the intercomparison cannot address surface albedo issue, since the Li algorithm does not include surface albedo as an input. Despite the problems in both data sets for the deserts, two types of estimates are coincidentally very close over these areas. One must be therefore cautious to assume that good agreement between two independent data sets gives more credit to the data.

In summary, the intercomparison study presented here allows identification of many deficiencies hidden in both satellite-based products under study, which may serve to guide the improvement of future SRB products. It is emphasized that the improvement should aim at coping with the problems identified, instead of being limited to the modification of wrong NSSR values, since the NSSR estimates can be correct but for the wrong reasons due to offsetting errors. For ISCCP/SRB, specific pending improvements include (1) angular correction over the geostationary satellite coverage, (2) spectral correction over highly reflective surfaces, (3) precipitable water amounts for deserts and highlands, and (4) computation of water vapor absorption. Many of these suggested improvements are being made by the WCRP/SRB working group and the upgraded ISCCP/SRB product will be released in the future. For ERBE/SRB it is recommended to (1) improve ERBE scene identification and angular correction over polar regions, (2) modify the algorithm to allow very low precipitable water, (3) use a more reliable scheme to compute water vapor absorption, and (4) account for aerosol effects explicitly. Although recommendations 2 and 3 have been incorporated into the revised algorithm [*Masuda*

et al., 1995], development of a new ERBE/SRB product is handicapped by the lack of aerosol climatology. This is because aerosol is subject to strong temporal and spatial variations and techniques of retrieving aerosol optical properties from space are still premature. This problem could be alleviated after the Earth Observation System commences near the end of the century, as the MODIS measurements are expected to provide quality aerosol data [*King et al.*, 1992]. Finally, for both ISCCP/SRB and ERBE/SRB, more reliable precipitable water retrieved from microwave measurements should be used when available.

Acknowledgments. The study benefits partly from preliminary work on the intercomparison led by T. Charlock, participated by R. Pinker, W. Staylor, C. Whitlock, W. Darnell, and the author. Informative discussions with R. Pinker and W. Rossow are gratefully acknowledged. T. Albert kindly provided the author with a two-dimensional Lagrangian interpolation scheme. The author also wishes to thank H. Barker for careful reviewing of the manuscript and L. Moreau and K. Masuda for providing some model results. The work is supported by the operating grant from the Canadian Green Plan to the Canada Centre for Remote Sensing.

References

Arino, O., G. Dedieu, and P. Y. Deschamps, Accuracy of satellite land surface reflectance determination, *J. Appl. Meteorol.*, *30*, 960–972, 1991.

Barker, H. W., and J. A. Davies, Multiple reflections across a linear discontinuity in surface albedo, *Int. J. Climatol.*, *9*, 203–214, 1989a.

Barker, H. W., and J. A. Davies, Surface albedo estimates from Nimbus-7 ERB data and a two-stream approximation of the radiative transfer equation, *J. Clim.*, *2*, 409–418, 1989b.

Barker, H. W., and Z. Li, Improved simulation of shortwave radiative transfer in the CCC GCM, *J. Clim.*, in press, 1994.

Barkstrom, B., E. Harrison, G. Smith, R. Green, J. Kibler, R. Cess, and the ERBE Science Team, Earth Radiation Budget Experiment (ERBE) archival and April 1985 results, *Bull. Am. Meteorol. Soc.*, *70*, 1254–1262, 1989.

Blanchet, J.-P., and R. List, Estimation of optical properties of Arctic haze using a numerical model, *Atmos. Ocean*, *21*, 444–465, 1983.

Cess, R., et al., Uncertainties in carbon dioxide radiative forcing in atmospheric general circulation models, *Sci.*, *262*, 1252–1255, 1993.

Charlock, T. P., C. H. Whitlock, and T. Alberta, The GEWEX Surface Radiation Budget project: Results available on line, *GEWEX News*, *3*(1) and (2), 1993. (Available from International GEWEX Project Office, Washington, D. C.)

D'Almeida, G. A., On the variability of desert aerosol radiative characteristics, *J. Geophys. Res.*, *92*, 3017–3026, 1987.

Darnell, W. L., W. F. Staylor, S. K. Gupta, N. A. Ritchey, and A. C. Wilber, Seasonal variation of surface radiation budget derived from International Satellite Cloud Climatology Project C1 data, *J. Geophys. Res.*, *97*, 15,741–15,760, 1992.

DiPasquale, R. C., and C. H. Whitlock, First WCRP long-term satellite estimates of surface solar flux for the global and selected regions, paper presented at the 25th International Symposium on Remote Sensing and Global Environmental Change, ERIM/JOANNEUM Res./CIESIN, Graz, Austria, April 4–8, 1993.

Fouquart, Y., B. Bonnel, and V. Ramaswamy, Intercomparison shortwave radiation codes for climate studies, *J. Geophys. Res.*, *96*, 8955–8968, 1991.

Fritz, S., P. Rao, and M. Weinstein, Satellite measurements of reflected solar energy and the energy received at the ground, *J. Atmos. Sci.*, *21*, 141–151, 1964.

Garratt, J. R., Incoming shortwave fluxes at the surface—A comparison of GCM results with observations, *J. Clim.*, *7*, 72–80, 1994.

King, M. D., Y. J. Kaufman, W. P. Menzel, and D. Tanre, Remote sensing of cloud, aerosol, and water vapour properties from the moderate resolution imaging spectrometer (MODIS), *IEEE Trans. Geosci. Remote Sens.*, *30*, 2–27, 1992.

Lacis, A. A., and J. E. Hansen, A parameterization for the absorption of solar radiation in the Earth's atmosphere, *J. Atmos. Sci.*, *31*, 118–132, 1974.

Li, Z., Retrieval of radiation budgets in the Arctic from satellite measurements, Ph.D. dissertation, 197 pp., Dep. of Atmos. and Oceanic Sci., McGill Univ., Montreal, 1991.

Li, Z., and H. Barker, Solar energy disposition: Intercomparison between satellite estimation, GCM simulation and surface observation, in IAMAS International Workshop on Clouds-Radiation Interactions and Their Parameterization in Climate Models, *WCRP-86*, WMO/*TD-648*, pp. 110–113, 1994.

Li, Z., and L. Garand, Estimation of surface albedo from space: A parameterization for global application, *J. Geophys. Res.*, *99*, 8335–8350, 1994.

Li, Z., and H. G. Leighton, Scene identification and its effect on cloud radiative forcing in the Arctic, *J. Geophys. Res.*, *96*, 9175–9188, 1991.

Li, Z., and H. G. Leighton, Narrowband to broadband conversion with spatially autocorrelated reflectance measurements, *J. Appl. Meteorol.*, *31*, 421–432, 1992.

Li, Z., and H. G. Leighton, Global climatology of solar radiation budgets at the surface and in the atmosphere from 5 years of ERBE data, *J. Geophys. Res.*, *98*, 4919–4930, 1993.

Li, Z., and H. G. Leighton, K. Masuda, and T. Takashima, Estimation of SW flux absorbed at the surface from TOA reflected flux, *J. Clim.*, *6*, 317–330, 1993a.

Li, Z., H. G. Leighton, and R. D. Cess, Surface net solar radiation estimated from satellite measurements: Comparison with tower observations, *J. Clim.*, *6*, 1764–1772, 1993b.

Li, Z., C. Whitlock, and T. Charlock, Assessment of the global monthly mean surface insolation estimated from satellite measurements using the Global Energy Balance Archive data, *J. Clim.*, *8*, 315–328, 1995.

Liu, W. T., W. Tang, F. J. Wentz, Precipitable water and surface humidity over global oceans from special sensor microwave image and European Center for Medium-Range Weather Forecasts, *J. Geophys. Res.*, *97*, 2251–2264, 1992.

Masuda, K., H. G. Leighton, and Z. Li, A new parameterization for the determination of solar flux absorbed at the surface from satellite measurements, *J. Clim.*, in press, 1995.

McClatchey, R. A., R. W. Fenn, J. E. A. Selby, F. E. Volz, and J. S. Garing, Optical Properties of the Atmosphere, 3rd ed., 110 pp., *Environ. Res. Pap. 411*, Air Force Cambridge Res. Lab., Bedford, Mass., 1972.

Ohmura, A., and H. Gilgen, *Global Energy Balance Archive (GEBA)*, 60 pp., Fachvereine, Zurich, 1991.

Ohmura, A., and H. Gilgen, Re-evaluation of the global energy balance, *Geophys. Monogr. Ser.* vol. 15, 75, edited by G. A. McBean and M. Hantel, pp. 93–110, 1993.

Pinker, R. T., and J. A. Ewing, Modeling surface solar radiation: Model formulation and validation, *J. Clim. Appl. Meteorol.*, *24*, 389–401, 1985.

Pinker, R., and I. Laszlo, Modelling surface solar irradiance for satellite applications on a global scale, *J. Appl. Meteorol.*, *31*, 194–211, 1992.

Pinker, R. T., R. Frouin, and Z. Li, A review of satellite methods to derive surface shortwave irradiance, *Remote Sens. Environ.*, *51*, 108–124, 1995.

Ramaswamy, V., and S. M. Freidenrecich, A study of broadband parameterizations of the solar radiative interactions with water vapor and water drops, *J. Geophys. Res.*, *97*, 11,487–11,512, 1992.

Schiffer, R. A., and W. B. Rossow, The International Satellite Cloud Climatology Project (ISCCP): The first project of the World Climate Research Programme, *Bull. Am. Meteorol. Soc.*, *64*, 779–984, 1983.

Schmetz, J., Towards a surface radiation climatology: Retrieval of downward irradiance from satellites, *Atmos. Res.*, *23*, 287–321, 1989.

Seager, R., and M. B. Blumenthal, Modeling tropical Pacific sea surface temperature with satellite derived solar radiative forcing, *J. Clim.*, *7*, 1943–1957, 1994.

Smith, G. L., R. N. Green, E. Raschke, M. Lee, J. T. Suttles, B. Wielicki, and R. Davies, Inversion methods for satellite studies of

the Earth's radiation budget: Development algorithms for the ERBE mission, *Rev. Geophys.*, *24*, 407–421, 1986.

Staylor, W. F., and A. C. Wilber, Global surface albedos estimated from ERBE data, in *Proceedings of the 7th AMS Conference on Atmospheric Radiation*, pp. 231–236, American Meteorological Society, Boston, Mass., 1990.

Suttles, J. T., and G. Ohring, Surface radiation budget for climate applications, *NASA Ref. Publ. 1169*, 132 pp., 1986.

Suttles, J. T., R. N. Green, P. Minnis, G. L. Smith, W. F. Staylor, B. A. Wielicki, I. J. Walker, D. F. Young, V. R. Taylor and L. L. Stowe, Angular Radiation Models for Earth-Atmosphere System, vol. 1, Shortwave Radiation, *NASA Ref. Publ. 1184*, 114 pp., 1988.

Vardavas, I. M., and K. Koutoulaki, A model for the solar radiation budget of the northern hemisphere: Comparison with ERBE data, *J. Geophys. Res.*, in press, 1995.

World Climate Project (WCP-55), *World Climate Research, Report of the Experts Meeting on Aerosols and Their Climatic Effects*, edited by A. Deepak and H. E. Gerber, 107 pp., Williamsburg, Va., 1983.

Whitlock, C. H., et al., Comparison of surface radiation budget satellite algorithms for downwelled shortwave irradiance with Wisconsin FIRE/SRB surface truth data, in *Proceedings of the 7th AMS Conference on Atmospheric Radiation*, pp. 237–242, American Meteorological Society, Boston, Mass., 1990.

Whitlock, C. H., T. P. Charlock, W. F. Staylor, R. T. Pinker, I. Laszlo, R. C. DiPasquale, and N. A. Ritchey, WCRP surface radiation budget shortwave data product description—Version 1.1, *NASA Tech. Memo. 107747*, 28 pp., 1993.

Wild, M., A. Ohmura, H. Gilgen, and E. Roeckner, Validation of general circulation models radiative fluxes using surface observations, *J. Clim.*, in press, 1995.

Z. Li, Canada Centre for Remote Sensing, 588 Booth, Ottawa, Ontario, Canada K1A 0Y7.

(Received April 12, 1994; revised September 1, 1994;
accepted October 5, 1994.)